Am J Transl Res 2017;9(3):971-985
www.ajtr.org /ISSN:1943-8141/AJTR0039381

Original Article

Activation of the α7 nicotinic receptor promotes lipopolysaccharide-induced conversion of M1 microglia to M2

Qichun Zhang[1,2,3], Ying Lu[3], Huimin Bian[3], Liwei Guo[1,2], Huaxu Zhu[1,2]

[1]Jiangsu Collaborative Innovation Center of Chinese Medicinal Resources Industrialization, [2]Jiangsu Botanical Medicine Refine Engineering Research Center, Nanjing University of Chinese Medicine, Nanjing 210023, PR China; [3]Department of Pharmacology, School of Pharmacy, Nanjing University of Chinese Medicine, Nanjing 210023, PR China

Received June 28, 2016; Accepted January 17, 2017; Epub March 15, 2017; Published March 30, 2017

Abstract: The α7 subtype of the nicotinic acetylcholine receptor (α7 nAChR) plays an essential role in the cholinergic anti-inflammatory pathway that regulates macrophage/microglia function in inflammation. Similar to M1 and M2 macrophages, M1 and M2 microglia exhibit pro-inflammation and anti-inflammation properties, respectively. In the present study, we analyzed function-associated phenotypes to detect the transformation of microglia with activation of α7 nAChRs. We used lentivirus-mediated shRNA to knockdown the expression of α7 nAChR in BV-2 microglia incubated with lipopolysaccharides (LPS, 0.1 μg/mL) and measured the acetylcholine (Ach, 1 μg/mL)-mediated release of cytokines, such as IL-1β, IL-4, IL-6, and IL-10, in the culture supernatant via radioimmunoassay. After stimulation with Ach, the expression of typical biomarkers for different microglia phenotypes, Iba-1 and Arg-1, was determined by cellular immunofluorescence. Furthermore, the expression of signaling molecules, including p38, JAK2/STAT3, PI3K/Akt and miR-124, was analyzed via western blotting and real-time PCR. We found that Ach inhibited LPS-induced IL-1β and IL-6 elevation and promoted IL-4 and IL-10 production and that knockdown of the α7 nAChR abolished these effects of Ach. In addition, Ach decreased LPS-induced Iba-1 expression and increased Arg-1 levels in an α7 nAChR-dependent manner. The LPS-inhibited activation of JAK2/STAT3 and PI3K/Akt was also rescued by Ach, an effect that was blocked by knockdown of the α7 nAChR. In contrast, Ach triggered the phosphorylation of JAK2 and STAT3 that was otherwise inactivated by LPS in BV-2 cells. Finally, the levels of miR-124 and downstream targets C/EBPα and PU.1 were significantly enhanced in LPS-treated BV-2 microglia, and the effect of Ach on this signaling pathway was blocked by α7 nAChR knockdown as expected. Overall, our data demonstrate that activation ofα7 nAChRs inhibits the transformation of M1 microglia and promotes the M2 phenotype, contributing to the modulation of vagus nerve neuroinflammation during several central nervous system diseases.

Keywords: Microglia, lipopolysaccharides, acetylcholine, α7 nAChR, polarization

Introduction

Microglia share several characteristics with the monocytes and macrophages of peripheral tissue, such as surface markers and receptors, and have been traditionally perceived as brain macrophages involved in the inflammatory response to pathogens. However, increasing evidence suggests microglia have additional novel functions beyond merely passive immune surveillance [1]. Microglia are a heterogeneous population of cells. Classically, resting microglia are activated to adopt the M1 phenotype by toxins, LPS and/or IFN-γ and secrete pro-inflammatory cytokines against pathogens and tumor cells. These cytokines also damage normal cellular residents, such as neurons and glial cells, especially during the uncontrolled chronic response. A well-known alternative to the primary M1 phenotype is M2, in which microglia secrete anti-inflammatory cytokines, such as IL-4 and IL-10, to rectify undesirable neuroinflammation and to repair damaged neurons. In addition to the modulation of neuroinflammation, M2 microglia with enhanced phagocytosis are responsible for the elimination of debris and misfolded proteins. Moreover, elevated neurogenesis and improvement of mem-

ory were observed in APP/PS1 mice upon treatment with IL-4 via activation of the M2 phenotype [2]. Therefore, given the distinct properties in biomarkers, morphology and function displayed by these microglial populations, it is an intriguing hypothesis that the activation of resting M2 microglia or the proper transition of M1 microglia to M2 would be expected to improve brain function under conditions of neurodegenerative disease, neuropsychiatric disorders or in the aftermath of acute cerebral vascular accidents.

In the last two decades, an emerging area of research focus has been the modulation of immune homeostasis by the nervous system, particularly the adrenergic nervous system, which maintains an "inflammatory reflex" by the prompt detection of systemic inflammatory stimuli by vagus afferents and delivery of signals to release acetylcholine (Ach) at the target location. In macrophages, the α7 subtype of the nicotinic acetylcholine receptor (α7 nAChR) was identified as a major component of the immune modulatory role of the cholinergic anti-inflammatory pathway [3, 4]. Both α7 nAChR knockout and blockade with specific antagonists abolish the anti-inflammatory effects of vagus nerve stimulation. The anti-inflammatory potential of Ach is mediated by inhibition of NF-κB via the STAT3 signaling pathway. Consistently, the phosphorylation of STAT3 at Tyr705 is commonly induced by LPS, a stimulator of macrophages [5]. Further investigation revealed that activated α7 nAChR induces microRNA-124 (miR-124), which is responsible for the inhibition of both STAT3 tyrosine phosphorylation and protein expression [6]. Microglia, the central nervous system (CNS) counterpart of macrophages in blood and peripheral tissue, are also regulated by signals from the vagus nerve following the activation of α7 nAChRs by Ach. MicroRNA-124 is abundantly expressed in the CNS, and in particular is highly expressed in resident microglia maintaining quiescence [7]. In addition, microRNA-124 downregulates the expression of the transcription factor C/EBP-α and its target PU.1, which play a key role in the maturation of microglia [8]. Moreover, activation of α7 nAChRs by Ach in microglia suppressed LPS-evoked TNF-α release. Several additional signaling pathways involving p44/42 and p38 mitogen activated protein kinases (MAPKs), JAK2/STAT3 and PLCC/InsP3/Ca^{2+} are also proposed to regulate the anti-inflammatory action of microglia [9].

While these studies demonstrate that Ach modulates LPS-stimulated microglial activation via α7 nAChRs, the role of this pathway in the homeostasis of microglia between resting, M1 and M2 phenotypesis still largely unknown. The aim of the present investigation was to explore the phenotypic regulation of microglia by Ach using LPS-induced M1 microglia and to determine the role of α7 nAChRs in the regulation of downstream signaling molecules.

Methods

BV-2 microglia cell culture

BV-2 cells from China Center for Type Culture Collection (Wuhan, China) were maintained in high glucose Dulbecco's Modified Eagle Medium (DMEM, Gibco, MA, USA) supplemented with 10% heat-inactivated fetal bovine serum (FBS, Gibco, MA, USA) and 100 mg/mL streptomycin and 100 U/mL penicillin in a humidified incubator with 95% air/5% CO_2 at 37°C. When the cells reached 70-80% confluence, they were detached with 0.1% trypsin-EDTA (Invitrogen, MA, USA) and seeded into the appropriate Petri dish or cell plate. Control BV-2s and those with α7 nAChR knockdown were cultured for 24 hrs and then starved for 2 hrs before treatment with 0.1 μg/mL LPS from *Escherichia coli* 0111:B4 (Sigma-Aldrich, Munich, Germany) and 1 μmol/L Ach (Sigma-Aldrich, Munich, Germany). Ach was added to the cells before or after the incubation of LPS, respectively, with a 30 min interval in between treatments.

RNAi of α7 nAChR

The knockdown of the α7 nAChR in BV-2 microglia was accomplished with α7nAChR shRNA (m) Lentiviral Particle Gene Silencers (sc-42533-V; Santa Cruz, TX, USA). BV-2 cells were seeded at 1×10^4 in 3 mm Petri dishes and incubated in DMEM with 10%FBS and antibiotics for 24 hrs before viral infection. The transfection solution was comprised of 10 μL of shRNA plasmid DNA (1 μg) and 4 μL of shRNA plasmid transfection reagent in 186 μL of transfection medium. When 50% confluent, the BV-2 cells were rinsed with transfection medium twice and incubated with transfection solution and DMEM

(1:5) for 5 hrs. After aspirating the transfection solution and rinsing with PBS two times, the BV-2 cells were subsequently incubated in DMEM with 20% FBS and antibiotics for 24 hrs. Following another 24 hrs in culture in DMEM with 10% FBS and antibiotics, the microglial cells successfully transfected with α7 nAChR shRNA plasmid were selected via puromycin treatment (4 μg/mL) for 72 hrs. The surviving and stable cells were collected and cultured extensively. The RNA level of α7 nAChR in both normal and α7 nAChR-knockdown cells was determined via real-time PCR with commercial primers.

Cellular immunofluorescence

BV-2 cells (1×10^5) were seeded in 12-well plates. After treatment with LPS and/or Ach for 24 hrs, the medium was aspirated. Then, the cells were covered with formaldehyde (4%) in warm PBS for 20 min at room temperature (RT). After aspirating the fixative, the BV-2 cells were rinsed three times in PBS for 5 min each and blocked with blocking buffer (5% goat serum and 0.3% Triton™ X-100 in PBS) for 60 min at RT. After aspiration of the blocking solution, the primary antibody diluted in PBS with 1% BSA and 0.3% Triton™ X-100 was applied to the cells and incubated at 4°C overnight. The next day, the cells were rinsed three times with PBS for 5 min each, then incubated with FITC-labeled secondary antibody for 1 hr at RT in the dark. The nuclei were stained by 4'6-diamidino-2-phenylindole (DAPI, Sigma-Aldrich, Munich, Germany), before obtaining images. Fluorescence was observed under a fluorescence microscope (Axio Observer Z1, Carl Zeiss).

Real-time PCR

The BV-2 cells treated with LPS for 12 hrs were harvested in 1 mL TRIzol (Invitrogen, MA, USA) according to the manufacturer's instructions. Phase separation was achieved by adding 0.2 mL chloroform and centrifugation at 12,000× g for 15 min at 4°C. The supernatant aqueous phase was collected and then mixed with isopropanol. After centrifugation at 12,000× g for 10 min at 4°C, the RNA pellet was harvested and further washed with 75% ethanol. Upon drying of ethanol, the RNA was resuspended in RNAase-free water. To measure α7 nAChR expression, the RNA was first reverse-transcribed with a TaqMan reverse transcription kit (Invitrogen, MA, USA) with reaction conditions of 37°C/15 min, 85°C/5 sec. The cDNA was mixed with gene-specific forward and reverse primers (5 pmol/μL) and extended with a PCR program on an ABI Prism 7500 machine (Applied Biosystems, MA, USA) according to the following program: 45°C/5 min-1 cycle; 94°C/30 sec-1 cycle; 94°C/5 sec, 60°C/30 sec-40 cycles, in a 25 μL reaction. SYBR Green oligonucleotides (Applied Biosystems, MA, USA) were used for detection and quantification of α7 nAChR mRNA levels, which were normalized to glyceraldehyde-3-phosphate dehydrogenase (GAPDH) levels using the $2^{-\Delta\Delta CT}$ method. The specificity of the PCR amplification was verified by melting curve analysis of the final products. Primer sequences used to amplify α7nAChR and GAPDH were as follows: F: 5'-AGCTGAGTGCAGGTGCTGG-3' and R: 5'-CAGGCCTCGGAAGCCAA-3' for α7 nAChR; F: 5'-ATTCAACGGCACAGTCAAGG-3' and R: 5'-TGGATGCAGGGATGATGTTC-3' for GAPDH [10]. For analysis of microRNA-124, the total RNA in the aqueous phase mixed with ethanol (half volume) was centrifuged at 10,000× g for 45 sec at 4°C through a HiBind RNA column. The flow through was collected and spun in a MicroElute RNA column following mixing with ethanol, and the column was further washed with SWB Wash buffer at 10,000× g for 60 sec at 4°C. Then, 25 μL DEPC-water (70°C) was added tothe microRNA-containing column and spun at 7,500× g for 30 sec. The concentration of microRNA was determined using a NanoDrop 2000 (Thermo Fisher Scientific, MA, USA). One-Step-qPCR SuperMix (TransGen Biotech, Beijing, China) was utilized to analyze the levels of microRNA-124 with the following program: 45°C/5 min-1 cycle; 94°C/30 sec-1 cycle; 94°C/5 sec, 60°C/30 sec-40 cycles, in a 20 μL reaction. The primers utilized are as follows: stem loop: 5'-CTCAACTGGTGTCGTGGAGTCGGCAATTCAGTTGAGGGCATTCA-3'; F: 5'-ACACTCCAGCTGGGTAAGGCACGCGGUT-3' and R: 5'-TGGTGTCGTGGAGTCG-3' for miR-124; F: 5'-CTCGCTTCGGCAGCACA-3' and R: 5'-AACGCTTCACGAATTTGCGT-3' for U6. The fluorescence labeling and calculations were consistent with a previous report.

Radioimmunoassay (RIA)

The levels of cytokines such as IL-1β, IL-6, IL-4 and IL-10 in the culture medium of BV-2 cells were analyzed with radioimmunoassay kits

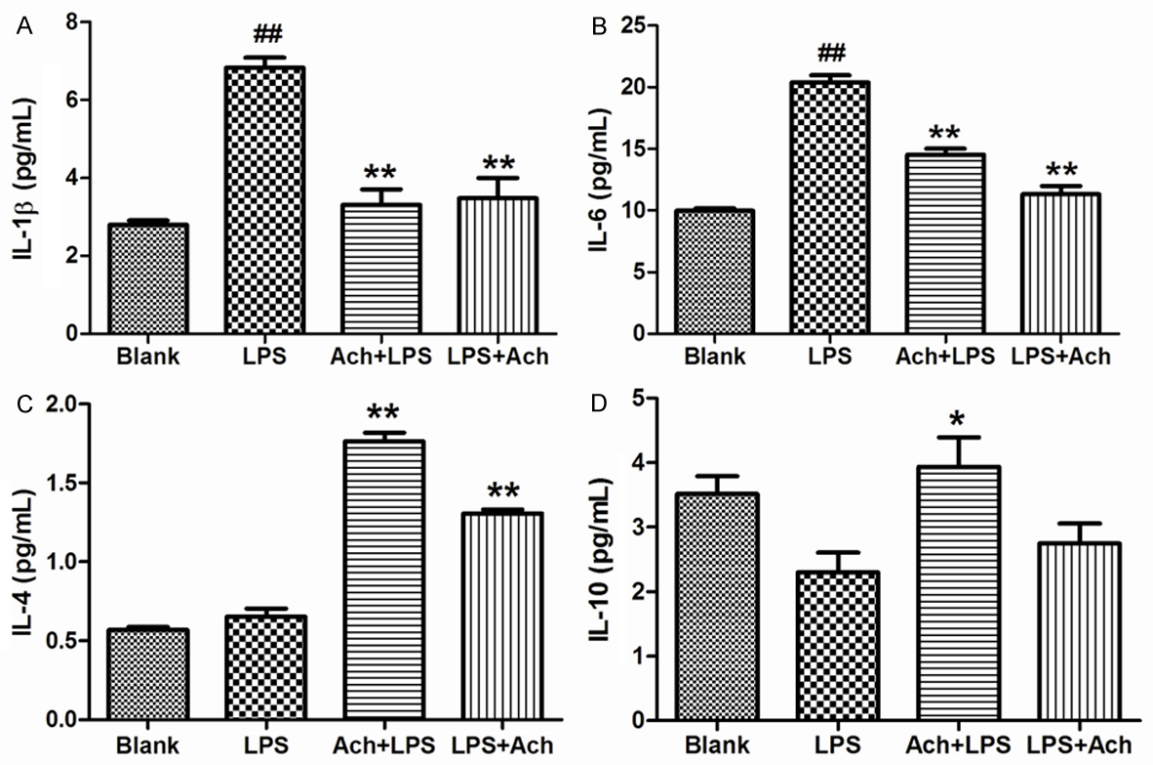

Figure 1. The effects of Ach on the secretion ofcytokines by microglia following stimulation with LPS. BV-2 cells were stimulated with LPS (100 ng/mL). Ach (1 μmoL) treatment was performed 30 min before or after the LPS stimulation. The levels of IL-1β (A), IL-6 (B), IL-4 (C), and IL-10 (D) in the culture medium of BV-2 cells were analyzed via RIA 24 hr after LPS incubation. Ach+LPS represents the condition with pretreatment of Ach 30 min before LPS stimulation, and LPS+Ach represents the condition with the treatment of Ach 30 min after LPS stimulation. All data are presented as the mean ± S.E.M., n = 6. ##P < 0.01, versus Blank; *P < 0.05, **P < 0.01 versus LPS.

(Sino-UK, Beijing, China) according to the protocols of the manufacturer. Briefly, the standard or samples were mixed with RIA buffer, antibodies and the corresponding ^{125}I-labeled cytokine and incubated at 4°C for 24 hrs. After mixing with polyethylene glycol and incubating for 15 min at RT, the assays were spun at 1,700× g for 15 min. The supernatant was aspirated and a γ-counter (911, Awareness Technology, FL, USA) was used to measure the counts per min (cpm) of the pellet. The concentration of cytokines was calculated according to a standard curve.

Western blotting

BV-2 cells treated with LPS and/or Ach were placed on ice and washed with ice-cold PBS. After removing the PBS, ice-cold lysis buffer (150 mM sodium chloride, 1.0% NP-40 or Triton X-100, 0.5% sodium deoxycholate, 0.1% sodium dodecyl sulfate, 50 mM Tris, pH 8.0) with ready-to-use cocktails of protease and phosphatase inhibitors (Thermo Fisher Scientific, MA, USA) was added and cells were collected using a cell scraper. After 30 min at 4°C, the supernatant of the lysate was collected via centrifugation at 12,000 rpm for 20 min and the protein concentration was determined via bicinchoninic acid (BCA) assay. Each sample was mixed with loading buffer (2×, 4% sodium dodecyl sulfate, 10% 2-mercaptoethanol, 20% glycerol, 0.004% bromophenol blue, 0.125 M Tris HCl, pH 6.8), boiled at 90°C for 5 min, and subsequently loaded (30 μg/per lane) and separated on a 10% sodium dodecyl sulfate-polyacrylamide gel (110 V), then transferred to polyvinylidenedifluoride membranes (Millipore, MA, USA, 90 V, 2 hrs, 4°C). The blotted membranes were blocked with 5% BSA for 1 hr, and incubated with primary antibody at 4°C overnight (p-p38 (Tyr182), p-JAK2 (Tyr1007), p-PI3K, p85a (Tyr508), p-Akt (Ser473)) and the conjugated appropriate secondary antibodies for 1 hr at RT. Then, the blotted proteins were detected by an enhanced chemiluminescence

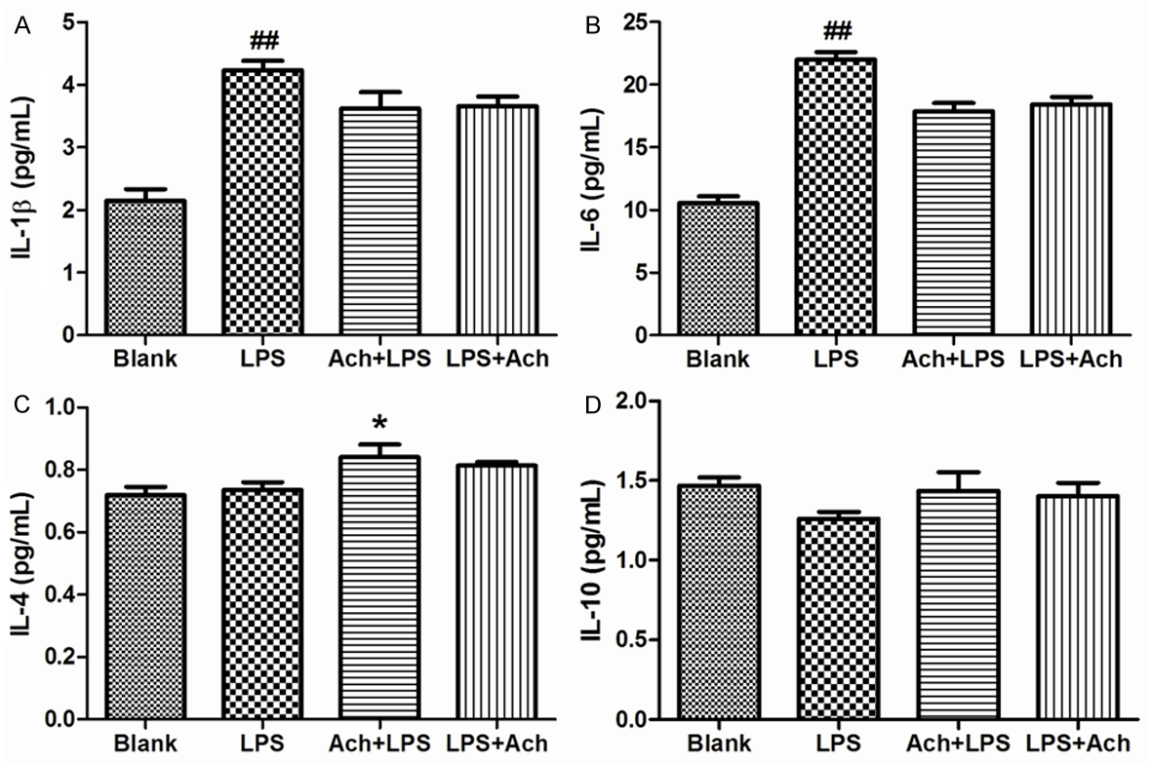

Figure 2. The effects of Ach on the LPS-induced secretion of cytokines by microglia with knockdown of α7 nAChRs. BV-2 cells stably transfected with α7 nAChR shRNA lentiviral particles were stimulated with LPS (100 ng/mL). Ach (1 μmoL) treatment was performed 30 min before or after the LPS stimulation. The levels of IL-1β (A), IL-6 (B), IL-4 (C), and IL-10 (D) in the cellular medium of BV-2 cells were analyzed via RIA 24 hrs after LPS incubation. Ach+LPS represents the condition with pretreatment of Ach 30 min before LPS stimulation, and LPS+Ach represents the condition with treatment of Ach 30 min after LPS stimulation. All data are presented as the mean ± S.E.M., n = 6. ##P < 0.01, versus Blank; *P < 0.05, versus LPS.

system. Immunoreactive bands were visualized by autoradiography, and the density of these bands was densitometrically quantified with a Gel Pro analyzer (Media Cybernetics, MD, USA).

Statistical analysis

Results are expressed as the means ± standard error and analyzed using a one-way ANOVA. A Newman-Keuls *post hoc* analysis was performed for pairwise multiple comparisons if significance was indicated by the ANOVA. The difference was considered to be statistically significant when $P < 0.05$.

Results

Ach modulates LPS-induced phenotype-associated cytokines in microglia

To determine the influence of Ach on the microglia phenotype under inflammation, the levels of phenotype-associated cytokines in the culture medium following LPS stimulation were analyzed via radioimmunoassay. As shown in **Figure 1**, LPS treatment strongly increased the release of IL-1β and IL-6 from microglia, indicative of the M1 phenotype. In contrast, M2 microglia-associated cytokines showed no change (IL-4) or a decrease in levels (IL-10) following LPS stimulation. Ach treatment prior to or following LPS stimulation significantly inhibited the LPS-induced increase in IL-1β and IL-6 and also enhanced the levels of IL-4. An increase in IL-10 secretion from microglia was apparent after pretreatment with Ach, but not when Ach treatment followed 30 min after LPS stimulation. These data demonstrate that Ach transforms LPS-activated M1 microglia to the M2 phenotype.

α7 nAChR mediates the effects of Ach on cytokines from microglia

Due to the pivotal role of α7 nAChRs in mediating the anti-inflammatory effects of Ach via

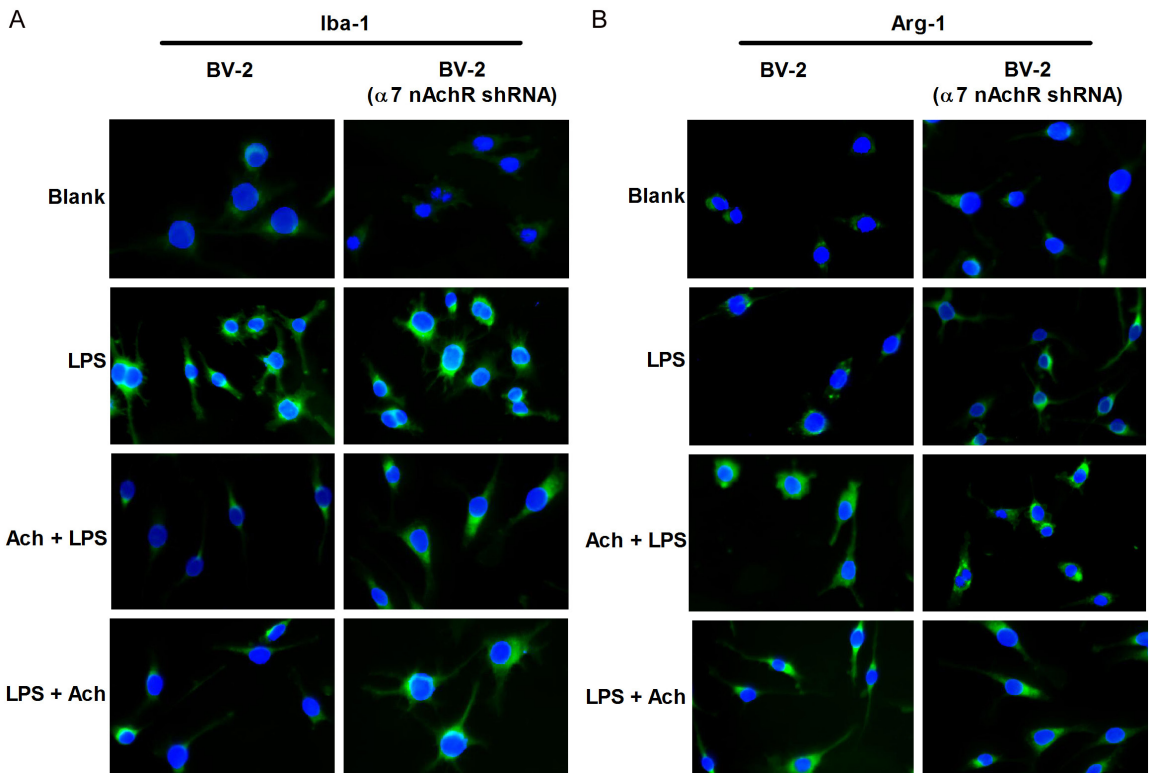

Figure 3. The effects of Ach on the protein levels of Iba-1 and Arg-1 in LPS-stimulated microglia with or without α7 nAChR knockdown. Ach (1 μmoL) treatment was performed 30 min before or after the LPS (100 ng/mL) stimulation. Iba-1 (A) and Arg-1 (B) were marked by primary antibodies and corresponding FITC-labeled secondary antibodies. The nucleus was stained by DAPI. The immunofluorescence was recorded via fluorescence microscopy 24 hrs following LPS stimulation.

regulation of immune responses of macrophages and microglia, we investigated the role of α7 nAChRs in mediating microglia phenotype by utilizing shRNA to knock down expression of α7nAChRs in microglia. Upon stimulation with LPS, the changes inIL-1β, IL-6, IL-4, and IL-10 secretion observed with the α7 nAChR knockdown microglia were similar to the results seen with control microglia (**Figure 2**). However, Ach failed to reverse the increase in LPS-evoked IL-1β and IL-6secretion by α7 nAChR knockdown microglia, likely due to the decreased expression of this receptor (**Figure 2A**, **2B**). Although a significant increase in IL-4 secretion was still observed with pretreatment of α7 nAChR knockdown microglia with Ach, the magnitude of the difference between LPS stimulation alone and Ach treatment +LPS stimulation was remarkably reduced compared with normal microglia (**Figure 2C**). In addition, the Ach-induced increase in IL-10 secretion was abolished in the nAChR α7 knockdown microglia (**Figure 2D**).

Ach inhibits the polarization of M1 microglia in anα7 nAChR-dependent manner

To further determine the phenotype of microglia induced by LPS with or without Ach, the expression of specific biomarkers of the M1 and M2 phenotype were explored via immunofluorescence. LPS stimulated the expression of Iba-1, the marker of M1 microglia, with more fluorescence intensity in both control and α7 nAChR knockdown BV-2 cells compared to untreated cells. In contrast, either pretreatment or post-treatment with Ach decreased the LPS-induced increase in Iba-1 expression in normal BV-2 cells, while the fluorescence intensity was not changed in the α7 nAChR knockdown microglia (**Figure 3A**). In parallel, we also analyzed the expression of Arg-1, a marker of M2 microglia. Low fluorescence related to Arg-1 expression was observed in microglia both with and without LPS stimulation. However, Ach treatment strikingly increased the levels of Arg-1, and this effect was largely abolished by

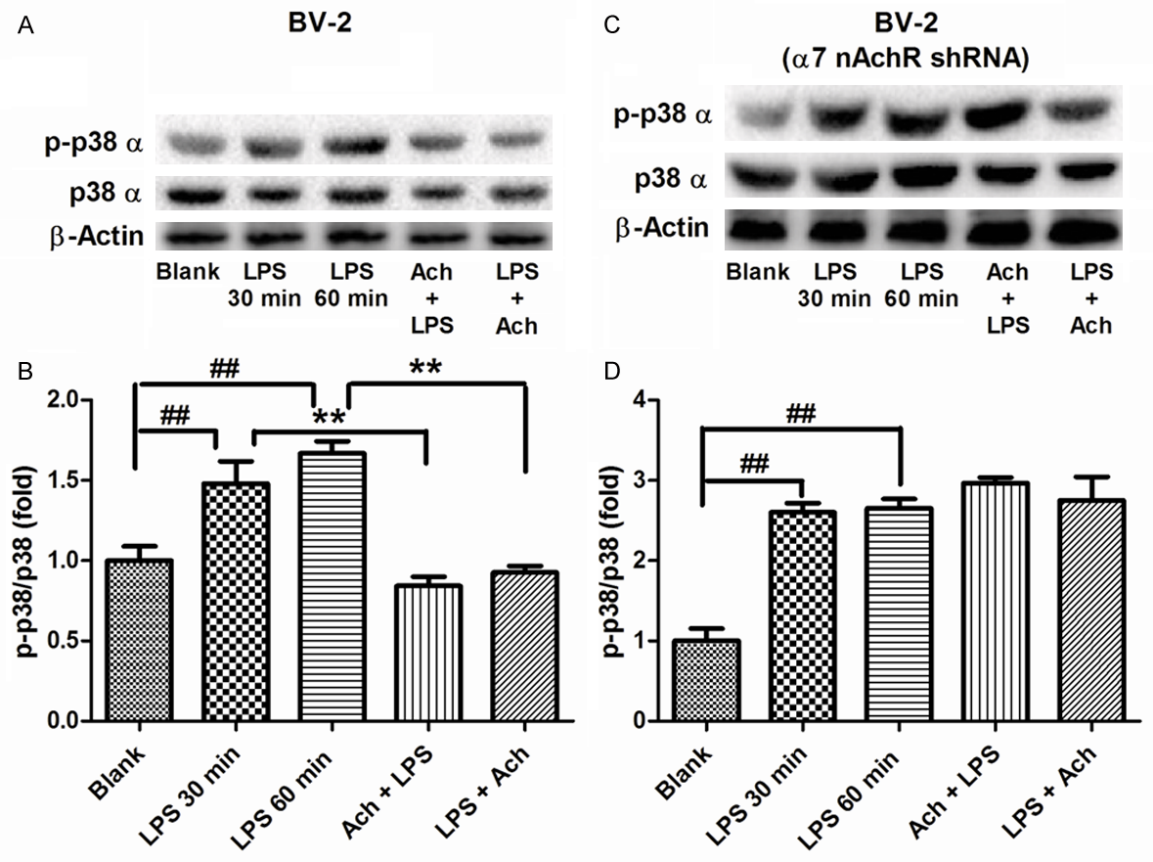

Figure 4. The effects of Ach on the activation of p38 MAPK in LPS-stimulated microglia with or without α7 nAChR knockdown. Ach (1 μmoL) treatment was performed 30 min before or after the LPS (100 ng/mL) stimulation. The levels of phosphorylated p38 MAPK and total p38 MAPK were detected at 30 and 60 min after LPS stimulation via Western blotting, corresponding to the two Ach treatment conditions: Ach+LPS (30 min) and LPS+Ach (60 min). All data are presented as the mean ± S.E.M., n = 3. ##P < 0.01; **P < 0.01.

RNAi of the α7 nAChR (**Figure 3B**). Thus, Ach prevents the LPS-induced polarization of M1 microglia and initiates activation of the alternative phenotype in an α7 nAChR-dependent manner.

Effects of Ach on signaling pathways downstream of the α7 nAChR

The signaling pathways responsible for the effects of Ach on microglia phenotype were subsequently determined. As shown in **Figure 4**, the activity of p38 MAPK, which is responsible for the activation of M1 microglia, was upregulated by stimulation with LPS. In contrast, Ach strongly inhibited the phosphorylation of p38 MAPK. Meanwhile, LPS-decreased phosphorylation of JAK2 and STAT3, which mediates the polarization of M2 microglia, was ameliorated by pretreatment or post-treatment with Ach (**Figure 5**). Although we did not detect significant activation of PI3K and Akt, components of a signaling pathway involved in the activation of JAK/STAT, in LPS-stimulated BV-2 cells, Ach did induce phosphorylation of both PI3K and Akt was in non-LPS-stimulated BV-2 cells (**Figure 6**). The modulation of p38 MAPK, JAK2/STAT3 and PI3K/Aktby Ach was blocked in α7 nAChR-knockdown BV-2 cells.

Effects of Ach on miR-124 levels and function in microglia

Based on the role of miR-124 in maintaining the naive microglial state, and the underlying association of this miRNA with α7 nAChR activation, the levels of miR-124 in BV-2 cells with and without Ach treatment were determined via real-time PCR. As shown in **Figure 7**, LPS stimulation led to a decrease in miR-124 levels, and either pretreatment or post-treatment with Ach blocked this LPS-induced decrease. The action

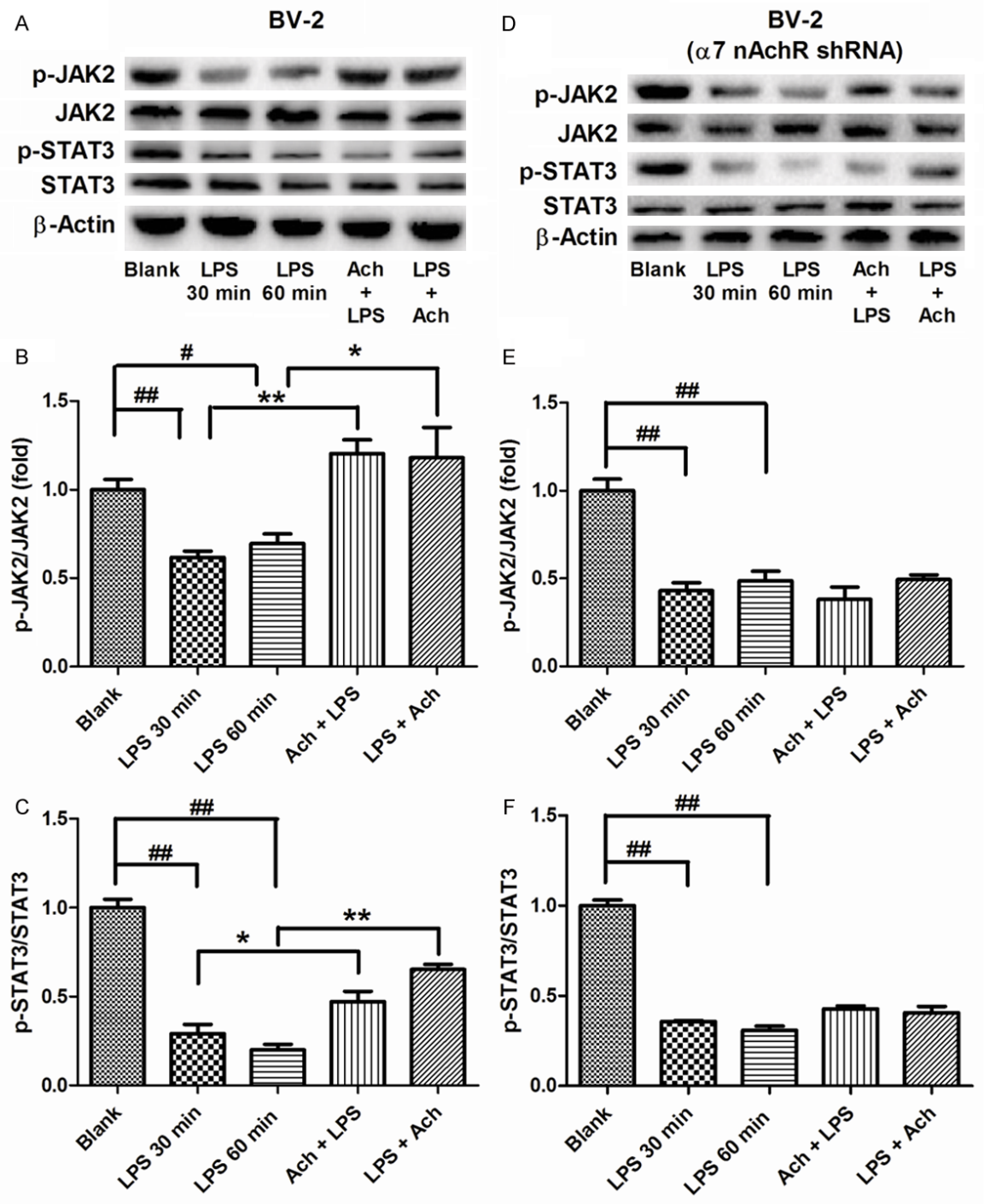

Figure 5. The effects of Ach on the JAK2/STAT3 signaling pathway in LPS-stimulated microglia with or without α7 nAChR knockdown. Ach (1 μmoL) treatment was performed 30 min before or after the LPS (100 ng/mL) stimulation. The levels of phosphorylated JAK2, phosphorylated STAT3 and total JAK2 and STAT3 were detected at 30 and 60 min after LPS stimulation via Western blotting, corresponding to the two Ach treatment conditions: Ach+LPS (30 min) and LPS+Ach (60 min). All data are presented as the mean ± S.E.M., n = 3. #P < 0.05; ##P < 0.01; *P < 0.05; **P < 0.01.

of Ach was attenuated in α7 nAChR-knockdown BV-2 cells. In addition, the expression of the transcription factor C/EBP-α, a known miR-124 target, was upregulated upon LPS-stimulated downregulation of miR-124. The expression of PU.1, a downstream target of C/EBP-α, was

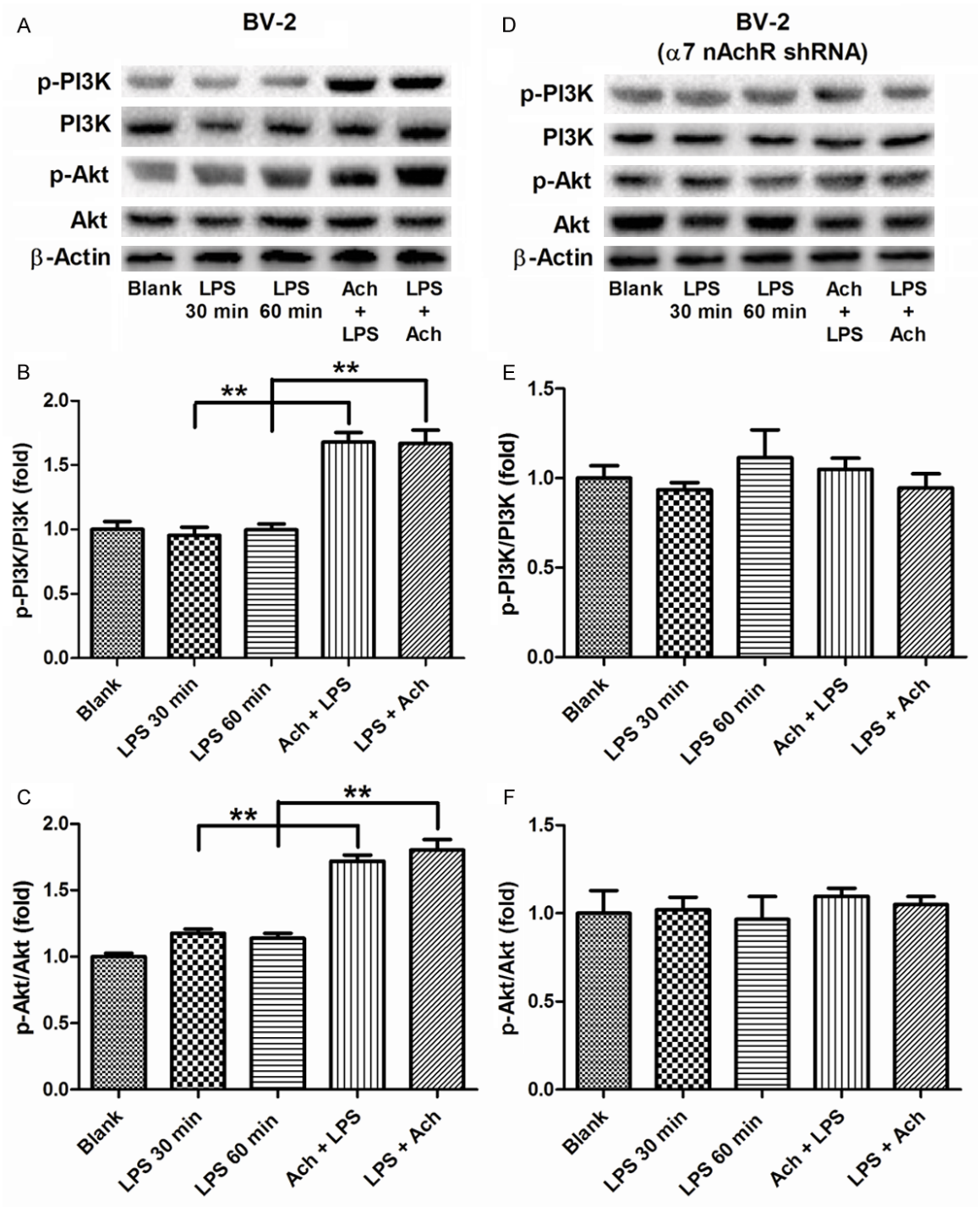

Figure 6. The effects of Ach on the signaling pathways of PI3K/Akt in LPS-stimulated microglia with or without α7 nAChR knockdown. Ach (1 μmoL) treatment was performed 30 min before or after the LPS (100 ng/mL) stimulation. The levels of phosphorylated PI3K, phosphorylated Akt, and total PI3K and Akt were detected at 30 and 60 min after LPS stimulation via Western blotting, corresponding to the two Ach treatment conditions: Ach+LPS (30 min) and LPS+Ach (60 min). All data are presented as the mean ± S.E.M., n = 3. ##P < 0.01; **P < 0.01.

also upregulated upon LPS stimulation, as expected. However, Ach treatment blocked the LPS-induced increase in C/EBP-α and PU.1, an effect that was lost in BV-2 cells α7 nAChR knockdown. Thus, Ach signals through α7 nAChRs to prevent the LPS-induced increase

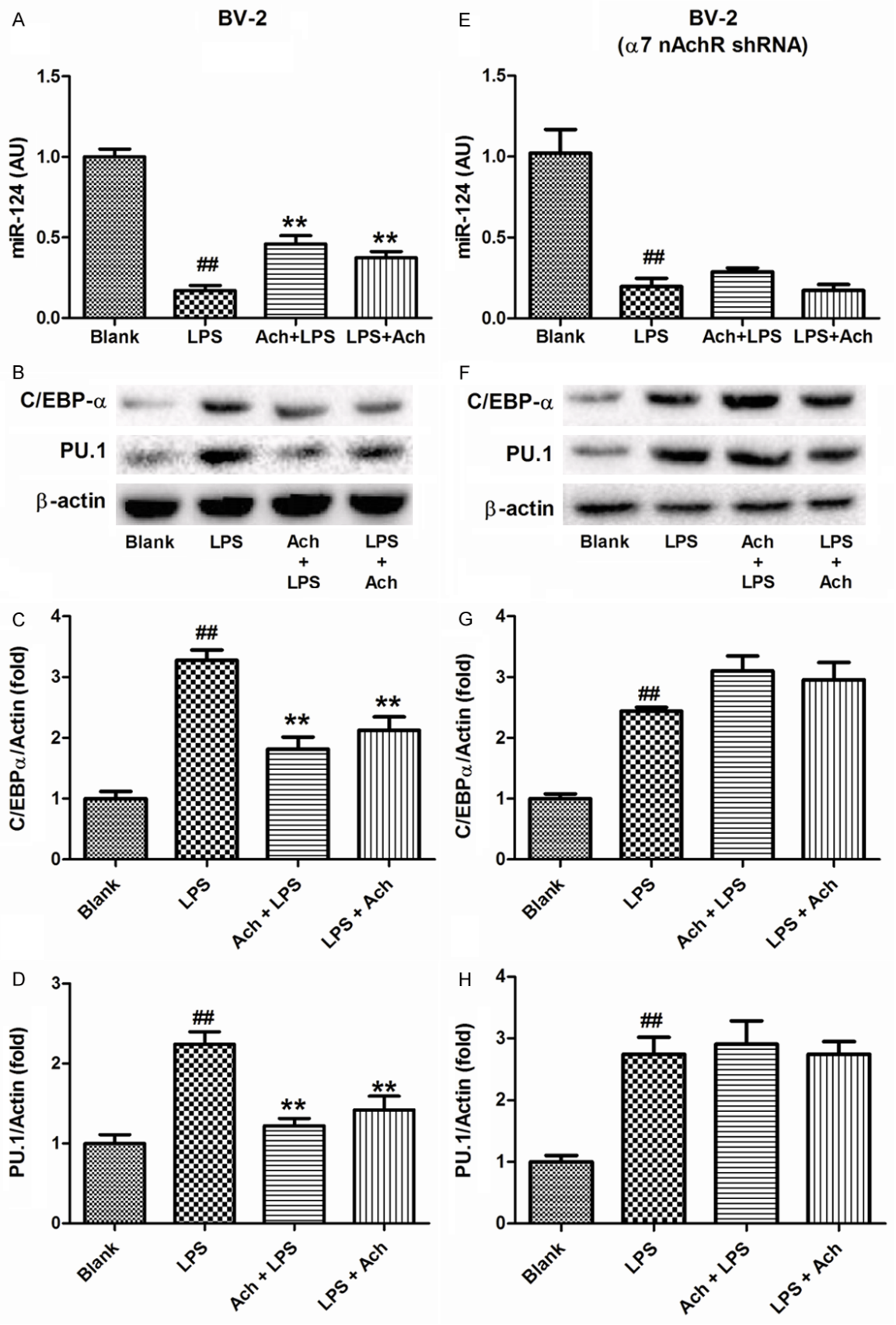
A
BV-2
miR-124 (AU)
1.5
1.0
0.5
0.0
##
**
**
Blank
LPS
Ach+LPS
LPS+Ach
E
BV-2
(α7 nAchR shRNA)
miR-124 (AU)
1.5
1.0
0.5
0.0
##
Blank
LPS
Ach+LPS
LPS+Ach
B
C/EBP-α
PU.1
β-actin
Blank
LPS
Ach + LPS
LPS + Ach
F
C/EBP-α
PU.1
β-actin
Blank
LPS
Ach + LPS
LPS + Ach
C
C/EBPα/Actin (fold)
4
3
2
1
0
##
**
**
Blank
LPS
Ach + LPS
LPS + Ach
G
C/EBPα/Actin (fold)
4
3
2
1
0
##
Blank
LPS
Ach + LPS
LPS + Ach
D
PU.1/Actin (fold)
3
2
1
0
##
**
**
Blank
LPS
Ach + LPS
LPS + Ach
H
PU.1/Actin (fold)
4
3
2
1
0
##
Blank
LPS
Ach + LPS
LPS + Ach

Figure 7. The effects of Ach on miR-124 and target proteins C/EBPα and PU.1 in LPS-stimulated microglia with or without α7 nAChR knockdown. Ach (1 μmoL) treatment was performed 30 min before or after the LPS (100 ng/mL) stimulation. After incubation with LPS for 12 hrs, miR-124 expression was analyzed with real-time PCR, and the expression of downstream proteins C/EBPα and PU.1 were assayed via western blotting. All data are presented as the mean ± S.E.M., n = 3. ##P < 0.01, versus Blank; **P < 0.01 versus LPS.

in C/EBP-α and PU.1 by maintaining the levels and function of miR-124.

Discussion

Microglia, an abundant cell population in the CNS, were originally characterized for their capacity to migrate and phagocytose. They arise from the mesodermal hematopoietic cells of the circulatory system and enter the CNS through the blood-brain barrier during perinatal stages [11]. Three types of microglia can be identified morphologically under different circumstances in the normal and injured brain: resting ramified, activated and amoeboid phagocytic, and each type represents a functionally distinct state [12]. Interestingly, the amoeboid phagocytic microglia are the predominant form in the perinatal brain, and these transform into resting ramified microglia with the development and maturation of the brain. However, several pathophysiological stimuli reversibly promote dynamic transformation from the ramified to the amoeboid state. These phenomena indicate that even the same type of microgliamay have a different significance in the developing brain compared to the brain during injury, infection, neuroinflammation or neurodegenerative disease [13]. Mature microglia expressa variety of macrophage-specific surface markers such as CD11b, scavenger receptors and Toll-like receptors, similar to other tissue-resident macrophages outside the CNS. The “inactive” and resting ramified microglia do not actually maintain quiescence but are engaged in immune surveillance to preserve the homeostasis in the nearby environment [14]. The classic phenotype of microglia, M1, is characterized by the production of TNF-α, IL-6, IL-1β and the membrane surface markerIba-1 upon stimulation with LPS. The cytokines secreted from activated microglia further promote the polarization of microglia into the M1 state through autocrine and paracrine signaling. The long-term pro-inflammatory state of M1 microglia disrupts the ability of these microglia to perform proper phagocytic functions and respond to anti-inflammatory signals. It was demonstrated that LPS inhibits microglial-mediated phagocytosis of Aβ protein, and the secretion of the associated cytokines IFN-γ and TNF-α prevents the degradation of internalized Aβ protein, thereby impairing the ability of M1 microglia to remove Aβ protein [15]. The LPS-induced inhibition of Aβ protein phagocytosis can be reversed by treatment with IL-4 and IL-10, the two representative cytokine markers of the alternative phenotype of microglia, M2, which upregulates the expression of scavenger receptors. Unlike the M1 phenotype, M2 microglia are defined as anti-inflammatory cells in the CNS, and these microglia express the specific marker Arg-1. Both IL-4 and IL-10, as well as some of the other marker proteins of M2 microglia, including Arg-1, MRC (CD206), CD163 and dectin-1 (Clec7A), are involved in the primary functions of M2 microglia. M2 microglia were demonstrated to play a role in the anti-inflammatory response, phagocytosis and the clearance of debris and misfolded proteins, wound repair and pro-neurogenic processes [15, 16]. The moderate inflammatory response in the brain affords fundamental protection for the CNS against external invaders and neurodegenerative conditions. Cytokines secreted from activated microglia, such as TNF-α, even acts as neuroprotective agents in stroke conditions [17]. However, a serious or long-term chronic inflammatory response commonly results in cellular damage, contributing to the development of neural autoimmune and neurodegenerative diseases. Therefore, the induction and maintenance of the M2 phenotype of microglia to treat pathological conditions in the CNS is an intriguing possibility. Rosiglitazone, an inducer of M2 microglia and macrophages, shows neuroprotective effects against traumatic brain injury, ischemia and spinal cord injury via the inhibition of neuroinflammation and reduced neuronal apoptosis and death [18-20]. Directintracerebral injection of the M2 microglia-derived cytokine IL-4 reduces amyloid β plaque load in the APP23 mouse model of Alzheimer’s disease, accompanied by improved cognition and the upregulation of Arg1- and YM1-positive M2 microglia. Similar results were obtained in 3-month-old APP/PS1 Alzheimer’s model mice [2, 21].

It is well-known that the vagus nerve has potentially positive anti-inflammatory actions via the regulation the function of immune cells, such as macrophages, through activation of nicotinic acetylcholine receptors. The α7 nAChR is the pivotal receptor that mediates the vagus nerve-inflammation reflex. Upon stimulation of α7 nAChRs, the STAT3 pro-survival pathway is activated, protecting against endoplasmic reticulum stress-induced M2 macrophage apoptosis [22]. In addition, STAT3 negatively regulates the inflammatory response as a transcription factor. The phosphorylation of STAT3 by the tyrosine kinase JAK2 promotes the expression of Src homology 2 domain protein (SOCS3), which binds to the glycoprotein 130 (GP130) subunit of the IL-6 receptor and inhibits TNF-α release via IL-6 signaling. Upon nicotine binding, JAK2 is recruited to the α7nAChR and then phosphorylated [23-25]. In the brain, cholinergic pathways confer anti-inflammatory properties on microglia via α7 nAChRs, with upregulation of COX-2 and prostaglandin E2 and suppression of LPS-evoked TNF-α secretion. Several signaling pathways mediated by proteins such as p44/42 and p38 MAPKs or JAK2/STAT3 are proposed to play a role in the activation of α7 nAChRs in microglia [9, 26]. Moreover, microRNAs are also emerging as regulators of immunity and inflammation, and modulate the Ach/α7 nAChR pathway. miR-132 targets and inhibits the mRNA encoding acetylcholinesterase (AChE), an Ach-degrading enzyme, leading to an increase in Ach and the anti-inflammatory effect of the neuroimmune axis [27]. Downstream in the Ach/α7 nAChR pathway, miR-124 inhibits both the tyrosine phosphorylation and protein expression of STAT3, which blocks the LPS-induced expression of IL-6 and TNF-α production. Unlike its role in the IL-6 receptor signaling pathway, STAT3 mediates LPS-induced IL-6 release [6]. Other well-characterized microRNAs in innate immunity are miR-146a and miR-155. miR-146a, an NF-κB-dependent gene, targets the signaling moleculesIL-1 receptor-associated kinase 1 and TNF receptor-associated factor 6, thereby limiting Toll-like receptor signaling [28]. miR-155 is expressed in a variety of immune cell types and targets the lipid phosphatase Src homology-2 domain-containing inositol 5-phosphatase 1 involved in macrophage activation [29]. Recent studies have identified that α7 nAChRs are not the sole contributor to immune regulation of the vagus nerve. The α4β nAChR, but not the α7nAChR, is expressed in alveolar macrophages [30]. In addition, α4β nAChR, rather than α7 nAChR, stimulates the recruitment of the GTPasedynamin-2 to the forming phagocytic cup and augments macrophage endocytosis and phagocytosis accompanied by the inhibition of immune activation in isolated intestinal and peritoneal macrophages [31]. α4β nAChRs in microglia/macrophages are supposed to play key roles in ischemia-initiated neuroinflammation [32].

In general, the immune-regulating actions of the efferent fibers of the vagus nerve are coordinated by the CNS in response to harmful peripheral stimuli or severe stress signaling through the afferent arm. First, the exciting afferents of the vagus nerve convey this stimulation and project to the brain stem, hypothalamus, hippocampus and forebrain. The immune regulation of microglia is inferred from this signal, which is commonly stimulated by positive and beneficial stimuli to rectify the hypofunction of the vagus nerve. For example, decreased cholinergic input to microglia in neurodegeneration is implicated in fuelling neuroinflammation [9]. In inflammatory bowel disease (IBD), decreased efferent vagus nerve activity is observed. In addition, the central activation of the efferent pathway reduced the level of major histocompatibility complex II and inhibited pro-inflammatory cytokine secretion from splenic $CD11c^{+}$ cells [33]. The bi-directional modulation of the vagus nerve connecting the brain and intestine may regulate both microglia and macrophages. IBD, typically a chronic systemic inflammation, initiates and hastens the progression of neurodegenerative diseases such as Alzheimer's disease. The inflammatory signal is transduced from the intestine to the brain, resulting in the polarization of resting microglia and further amplifying the cascade response, which is the pivotal pathological mechanism in IBD-associated CNS disorders [34, 35]. As a result of the dysbiosis in IBD, more pro-inflammatory cytokines, microbial metabolites, neuroactive substances and polysaccharides directly act on the brain through the circulatory system or through initial stimulation of the intestinal immune system and enteric nervous system and subsequent projection to the brain. Alteration of this microbial imbalance with probiotics or the enhance-

ment of beneficial metabolites such as short-chain fatty acids (SCFAs) facilitates the amelioration of IBD and related CNS disorders in emotion, memory and behavior. The SCFA butyrate has a direct effect on afferent terminals [36]. Hydrogen sulfide (H_2S), an important gasotransmitter produced by the sulfate-reducing bacteria in the colon is increased in IBD, but administration of H_2S donors reduces inflammatory conditions. Similar to the effect of SCFAs, this induces hypersensitivity of rat capsaicin-sensitive lung vagus neurons through transient receptor potential ankyrin 1 [37, 38]. Therefore, the enhancement of vagus nerve signals with external stimuli potentially has a favorable effect not only on chronic systemic inflammation, such as IBD and rheumatoid arthritis, but also on microglia-associated neuroinflammation. Modulation of microglia phenotypes via specific AChRs, direct electrical stimulation of the vagus nerve promoting microglia functional differences and external substances of interest, such as SCFAs, H_2S donors, probiotics, can induce a significant electrophysiological signal. The modulation of microglia by the vagus nerve displays more practical value until all the three questions are answered and identified.

In the present investigation, Ach prevented the LPS-evoked classical activation of microglia and promoted alternative activation, as assessed by the modulation of cytokines and markers. Three units of the MAPK signaling pathway involved in this phenotypic regulation activated by LPS promoted polarization of M1 microglia and were blocked by Ach. Both direct blockade with Ach and a decrease in M1 microglia are responsible for the deactivation of p38 MAPK. Moreover, Ach stimulated the JAK2/STAT3 signaling pathway, which has been reported to be involved in the alternative activation of macrophages, namely, M2 macrophages, induced by IL-4 and might contribute to the alternative activation of microglia. However, it remains unknown whether the M2 microglia were derived from resting microglia or the M1 phenotype. The third associated component of this pathway was miR-124 and its downstream targets C/EBP-α and PU.1, which regulate microglial quiescence. Ach-induced enhancement of miR-124 expression impeded the LPS-initiated classical activation of microglia.

In summary, Ach promoted the transformation of M1 microglia to the M2 phenotype through the JAK2/STAT3 pathway by activation of α7 nAChRs. Moreover, Ach-maintained miR-124 inhibited LPS-induced polarization of naïve microglia via C/EBPα and PU.1. These two mechanisms modulated microglia phenotype and function, which contributes to the neuroinflammatory response under conditions of cerebral disease.

Acknowledgements

This research was financially supported by the Administration of Traditional Chinese Medicine of Jiangsu Province [Project No. LZ13007]; National Natural Science Foundation of China [Project No. 81573635; 30873450]; A Project Funded by Natural Science Foundation of Jiangsu Province [Project No. BK 2012855; BY 2012036]; A Project Funded by Innovation Research Team of Nanjing University of Chinese Medicine; A Project Funded by the Six Talent Project in Jiangsu Province; and A Project Funded by the Priority Academic Program Development of Jiangsu Higher Education Institutions (PAPD).

Disclosure of conflict of interest

None.

Address correspondence to: Dr. Huaxu Zhu, Jiangsu Collaborative Innovation Center of Chinese Medicinal Resources Industrialization, Nanjing University of Chinese Medicine, 138 Xianlin Rd., Nanjing 210023, PR China. Tel: +862585811070; Fax: +862585811067; E-mail: zhuhx@njucm.edu.cn

References

[1] Cherry JD, Olschowka JA and O'Banion MK. Neuroinflammation and M2 microglia: the good, the bad, and the inflamed. J Neuroinflammation 2014; 11: 98.

[2] Kiyota T, Okuyama S, Swan RJ, Jacobsen MT, Gendelman HE and Ikezu T. CNS expression of anti-inflammatory cytokine interleukin-4 attenuates Alzheimer's disease-like pathogenesis in APP+PS1 bigenic mice. FASEB J 2010; 24: 3093-3102.

[3] Wang H, Liao H, Ochani M, Justiniani M, Lin X, Yang L, Al-Abed Y, Wang H, Metz C, Miller EJ, Tracey KJ and Ulloa L. Cholinergic agonists inhibit HMGB1 release and improve survival

in experimental sepsis. Nat Med 2004; 10: 1216-1221.
[4] Wang H, Yu M, Ochani M, Amella CA, Tanovic M, Susarla S, Li JH, Wang H, Yang H, Ulloa L, Al-Abed Y, Czura CJ and Tracey KJ. Nicotinic acetylcholine receptor alpha7 subunit is an essential regulator of inflammation. Nature 2003; 421: 384-388.
[5] Pena G, Cai B, Liu J, van der Zanden EP, Deitch EA, de Jonge WJ and Ulloa L. Unphosphorylated STAT3 modulates alpha 7 nicotinic receptor signaling and cytokine production in sepsis. Eur J Immunol 2010; 40: 2580-2589.
[6] Sun Y, Li Q, Gui H, Xu DP, Yang YL, Su DF and Liu X. MicroRNA-124 mediates the cholinergic anti-inflammatory action through inhibiting the production of pro-inflammatory cytokines. Cell Res 2013; 23: 1270-1283.
[7] Cheng LC, Pastrana E, Tavazoie M and Doetsch F. miR-124 regulates adult neurogenesis in the subventricular zone stem cell niche. Nat Neurosci 2009; 12: 399-408.
[8] Ponomarev ED, Veremeyko T, Barteneva N, Krichevsky AM and Weiner HL. MicroRNA-124 promotes microglia quiescence and suppresses EAE by deactivating macrophages via the C/EBP-alpha-PU.1 pathway. Nat Med 2011; 17: 64-70.
[9] Kawamata J and Shimohama S. Stimulating nicotinic receptors trigger multiple pathways attenuating cytotoxicity in models of Alzheimer's and Parkinson's diseases. J Alzheimers Dis 2011; 24 Suppl 2: 95-109.
[10] Fan YY, Zhang ST, Yu LS, Ye GH, Lin KZ, Wu SZ, Dong MW, Han JG, Feng XP and Li XB. The time-dependent expression of alpha7nAChR during skeletal muscle wound healing in rats. Int J Legal Med 2014; 128: 779-786.
[11] Lawson LJ, Perry VH, Dri P and Gordon S. Heterogeneity in the distribution and morphology of microglia in the normal adult mouse brain. Neuroscience 1990; 39: 151-170.
[12] Ling EA and Wong WC. The origin and nature of ramified and amoeboid microglia: a historical review and current concepts. Glia 1993; 7: 9-18.
[13] Zhang SC, Goetz BD, Carre JL and Duncan ID. Reactive microglia in dysmyelination and demyelination. Glia 2001; 34: 101-109.
[14] Nimmerjahn A, Kirchhoff F and Helmchen F. Resting microglial cells are highly dynamic surveillants of brain parenchyma in vivo. Science 2005; 308: 1314-1318.
[15] Koenigsknecht-Talboo J and Landreth GE. Microglial phagocytosis induced by fibrillar beta-amyloid and IgGs are differentially regulated by proinflammatory cytokines. J Neurosci 2005; 25: 8240-8249.
[16] Martinez FO, Helming L and Gordon S. Alternative activation of macrophages: an immunologic functional perspective. Annu Rev Immunol 2009; 27: 451-483.
[17] Sriram K, Matheson JM, Benkovic SA, Miller DB, Luster MI and O'Callaghan JP. Deficiency of TNF receptors suppresses microglial activation and alters the susceptibility of brain regions to MPTP-induced neurotoxicity: role of TNF-alpha. FASEB J 2006; 20: 670-682.
[18] Yi JH, Park SW, Brooks N, Lang BT and Vemuganti R. PPARgamma agonist rosiglitazone is neuroprotective after traumatic brain injury via anti-inflammatory and anti-oxidative mechanisms. Brain Res 2008; 1244: 164-172.
[19] Lee CH, Park OK, Yoo KY, Byun K, Lee B, Choi JH, Hwang IK, Kim YM and Won MH. The role of peroxisome proliferator-activated receptor gamma, and effects of its agonist, rosiglitazone, on transient cerebral ischemic damage. J Neurol Sci 2011; 300: 120-129.
[20] Zhang Q, Hu W, Meng B and Tang T. PPARgamma agonist rosiglitazone is neuroprotective after traumatic spinal cord injury via anti-inflammatory in adult rats. Neurol Res 2010; 32: 852-859.
[21] Kawahara K, Suenobu M, Yoshida A, Koga K, Hyodo A, Ohtsuka H, Kuniyasu A, Tamamaki N, Sugimoto Y and Nakayama H. Intracerebral microinjection of interleukin-4/interleukin-13 reduces beta-amyloid accumulation in the ipsilateral side and improves cognitive deficits in young amyloid precursor protein 23 mice. Neuroscience 2012; 207: 243-260.
[22] Lee RH and Vazquez G. Evidence for a prosurvival role of alpha-7 nicotinic acetylcholine receptor in alternatively (M2)-activated macrophages. Physiol Rep 2013; 1: e00189.
[23] de Jonge WJ, van der Zanden EP, The FO, Bijlsma MF, van Westerloo DJ, Bennink RJ, Berthoud HR, Uematsu S, Akira S, van den Wijngaard RM and Boeckxstaens GE. Stimulation of the vagus nerve attenuates macrophage activation by activating the Jak2-STAT3 signaling pathway. Nat Immunol 2005; 6: 844-851.
[24] Welte T, Zhang SS, Wang T, Zhang Z, Hesslein DG, Yin Z, Kano A, Iwamoto Y, Li E, Craft JE, Bothwell AL, Fikrig E, Koni PA, Flavell RA and Fu XY. STAT3 deletion during hematopoiesis causes Crohn's disease-like pathogenesis and lethality: a critical role of STAT3 in innate immunity. Proc Natl Acad Sci U S A 2003; 100: 1879-1884.
[25] Yasukawa H, Ohishi M, Mori H, Murakami M, Chinen T, Aki D, Hanada T, Takeda K, Akira S, Hoshijima M, Hirano T, Chien KR and Yoshi-

mura A. IL-6 induces an anti-inflammatory response in the absence of SOCS3 in macrophages. Nat Immunol 2003; 4: 551-556.
[26] De Simone R, Ajmone-Cat MA, Carnevale D and Minghetti L. Activation of alpha7 nicotinic acetylcholine receptor by nicotine selectively up-regulates cyclooxygenase-2 and prostaglandin E2 in rat microglial cultures. J Neuroinflammation 2005; 2: 4.
[27] Shaked I, Meerson A, Wolf Y, Avni R, Greenberg D, Gilboa-Geffen A and Soreq H. MicroRNA-132 potentiates cholinergic anti-inflammatory signaling by targeting acetylcholinesterase. Immunity 2009; 31: 965-973.
[28] Taganov KD, Boldin MP, Chang KJ and Baltimore D. NF-kappaB-dependent induction of microRNA miR-146, an inhibitor targeted to signaling proteins of innate immune responses. Proc Natl Acad Sci U S A 2006; 103: 12481-12486.
[29] O'Connell RM, Chaudhuri AA, Rao DS and Baltimore D. Inositol phosphatase SHIP1 is a primary target of miR-155. Proc Natl Acad Sci U S A 2009; 106: 7113-7118.
[30] Matsunaga K, Klein TW, Friedman H and Yamamoto Y. Involvement of nicotinic acetylcholine receptors in suppression of antimicrobial activity and cytokine responses of alveolar macrophages to Legionella pneumophila infection by nicotine. J Immunol 2001; 167: 6518-6524.
[31] van der Zanden EP, Snoek SA, Heinsbroek SE, Stanisor OI, Verseijden C, Boeckxstaens GE, Peppelenbosch MP, Greaves DR, Gordon S and De Jonge WJ. Vagus nerve activity augments intestinal macrophage phagocytosis via nicotinic acetylcholine receptor alpha4beta2. Gastroenterology 2009; 137: 1029-1039, 1039, e1021-1024.
[32] Martin A, Szczupak B, Gomez-Vallejo V, Domercq M, Cano A, Padro D, Munoz C, Higuchi M, Matute C and Llop J. In vivo PET imaging of the alpha4beta2 nicotinic acetylcholine receptor as a marker for brain inflammation after cerebral ischemia. J Neurosci 2015; 35: 5998-6009.
[33] Ji H, Rabbi MF, Labis B, Pavlov VA, Tracey KJ and Ghia JE. Central cholinergic activation of a vagus nerve-to-spleen circuit alleviates experimental colitis. Mucosal Immunol 2014; 7: 335-347.
[34] Perry VH, Newman TA and Cunningham C. The impact of systemic infection on the progression of neurodegenerative disease. Nat Rev Neurosci 2003; 4: 103-112.
[35] Wang Y and Kasper LH. The role of microbiome in central nervous system disorders. Brain Behav Immun 2014; 38: 1-12.
[36] Lal S, Kirkup AJ, Brunsden AM, Thompson DG and Grundy D. Vagal afferent responses to fatty acids of different chain length in the rat. Am J Physiol Gastrointest Liver Physiol 2001; 281: G907-915.
[37] Flannigan KL, Agbor TA, Blackler RW, Kim JJ, Khan WI, Verdu EF, Ferraz JG and Wallace JL. Impaired hydrogen sulfide synthesis and IL-10 signaling underlie hyperhomocysteinemia-associated exacerbation of colitis. Proc Natl Acad Sci U S A 2014; 111: 13559-13564.
[38] Hsu CC, Lin RL, Lee LY and Lin YS. Hydrogen sulfide induces hypersensitivity of rat capsaicin-sensitive lung vagal neurons: role of TRPA1 receptors. Am J Physiol Regul Integr Comp Physiol 2013; 305: R769-779.